

SUBMILLIMETER EMISSION FROM L1641 AND THE ORION NEBULA

J. SMITH,¹ D. K. LYNCH,^{1,2} D. CUDABACK,² AND M. W. WERNER¹

Received 1979 April 19; accepted 1979 June 26

ABSTRACT

Submillimeter continuum emission from a $40' \times 25'$ portion of L1641 containing the Orion Nebula has been mapped at $400 \mu\text{m}$ with 3.0 resolution. The observed submillimeter radiation is produced by thermal emission from dust associated with the well-studied molecular clouds in this region. The dust column densities derived from the submillimeter observations show that L1641 contains a dense core oriented north-south and about $30' \times 5'$ in extent. The submillimeter continuum observations are compared with molecular line emission observations to obtain additional information about the structure of the region and about the properties of the dust.

Subject headings: infrared: sources — interstellar: molecules — nebulae: Orion Nebula

I. INTRODUCTION

This paper reports the first results of a low-spatial-resolution survey of submillimeter continuum emission from dust clouds. Regions about one-half square degree in extent which exhibit extensive molecular emission and contain sites of recent and ongoing star formation were chosen for this survey. The angular resolution (3.0) and the spatial extent of the present submillimeter measurements are comparable to the values characteristic of radio continuum and molecular line studies. Therefore these observations provide data on the interstellar dust which complement the observations of the interstellar gas within these regions.

The present paper reports observations of the central region of the L1641 dust cloud (Lynds 1962). Kutner *et al.* (1977) have shown that L1641 is part of a giant molecular cloud complex about 18 square degrees in extent with a total mass of about $10^5 M_{\odot}$ and a mean molecular column density $N_{\text{H}_2} \sim 5 \times 10^{21} \text{ cm}^{-2}$. Within L1641, Kutner, Evans, and Tucker (1976) have discovered a dense core about $30'$ in north-south extent that is bounded by the H II regions M42 to the south, M43 to the east, and NGC 1977 to the north. This core contains three distinct local maxima in the ^{12}CO ($J = 1-0$) radiation temperature. These are Orion Molecular Cloud 1 (OMC-1) near the Orion Nebula, OMC-2 which lies $\sim 12'$ N of OMC-1, and a third bright region $\sim 16'$ N of OMC-2 which will be referred to as OMC-3. The dense core of OMC-1 contains a cluster of infrared stars with $L \gtrsim 10^5 L_{\odot}$ which are believed to be protostars or pre-main-sequence objects. Located near OMC-2 is a lower-luminosity infrared cluster. OMC-1 has been studied extensively at infrared and radio wavelengths (see Werner, Becklin, and Neugebauer 1977, and references therein). There are less complete analyses of OMC-2 and of the region connecting OMC-2 and

OMC-3 with OMC-1 (Gatley *et al.* 1974; Fazio *et al.* 1974; Thronson *et al.* 1978; Werner *et al.* 1980; Keene *et al.* 1980).

Previous submillimeter observations of the L1641 region have been limited to maps of the central few arcminutes of OMC-1 and measurements at single points in the OMC-2 and OMC-3 regions (Harper *et al.* 1972; Gezari *et al.* 1974; Soifer and Hudson 1974; Hudson and Soifer 1976; Thronson *et al.* 1978). The present observations delineate the distribution of continuum emission from dust over a $40' \times 25'$ region containing OMC-1, OMC-2, and OMC-3. The principal observed feature is a continuous, well-defined ridge of submillimeter emission which extends from OMC-1 to near OMC-3, some $28'$ (4 pc) to the north.

These are the first results obtained from a submillimeter observatory operated jointly by the California Institute of Technology and the University of California at Berkeley. This facility and the observational techniques are described in § II, and the results of the observations are presented in § III. Section § IV includes discussion of the distribution of mass as inferred from the submillimeter observations, an estimate of the properties of the emitting grains, and a brief discussion of the energetics of the source. The main conclusions are summarized in § V.

II. OBSERVATIONS

The submillimeter observations were made between 1976 November and 1978 April at the Caltech-University of California at Berkeley submillimeter observatory. This observatory consists of a 1.6 m diameter, $f/1.0$ telescope (Neugebauer and Leighton 1969) located at an altitude of 3.9 km on White Mountain in central California. During the past 2 years this facility has been used both for scientific observations and for a systematic investigation of the properties of the White Mountain site for submillimeter astronomy. The results of the site survey will be presented by Smith, Cudaback, and Lynch (1980).

For the observations described here, the spectral

¹ Department of Physics, California Institute of Technology.
² Radio Astronomy Laboratory, University of California, Berkeley.

bandpass is determined by a combination of the response of the detector system and the transmission of the atmosphere. The detector is a liquid-helium-cooled composite bolometer (Hauser and Notaries 1975), which is measured to have a spectral response which is approximately wavelength-independent. The filtering consists of 1.0 mm of Fluorogold (Muehler and Weiss 1973) at a temperature of 1.5 K, 1.0 mm of black polyethylene attached to the radiation shield, and 3.0 mm of Teflon which was used for the dewar window. This filtering and the Earth's atmospheric transmission produce the short-wavelength cutoff at $\lambda \sim 300 \mu\text{m}$, and diffraction at the 1.5 mm focal plane aperture provides the long-wavelength cutoff beyond $\lambda \sim 1000 \mu\text{m}$. For typical observing conditions with $\lesssim 2 \text{ mm}$ of line-of-sight precipitable water vapor, and a cosmic source spectrum $F_\nu \propto \nu^3$ to ν^4 , the system has an effective wavelength between 380 and 420 μm ; a mean value of 400 μm is adopted for the present analysis. This broad-band system was used for the mapping observations which are the main results of the present paper. Some narrow-band measurements were made using a wire mesh interference filter ($\lambda/\Delta\lambda = 10$, $\lambda_0 = 340 \mu\text{m}$) placed external to the dewar. All measurements have been made by beam switching. Sky emission is subtracted by oscillating the telescope primary mirror east-west at 20 Hz with a 5' amplitude. The beam shape, determined from scans of the planets, is Gaussian with full width at half-maximum of 3'.0.

The map of the submillimeter emission was constructed from a series of photometric measurements made with the broad-band system. The entire region within the lowest contour of Figure 2 was sampled at single beam (3'.0) spacing, and half-beam spacing was used near the peak of OMC-1 and along the central north-south ridge (Fig. 4a). In addition, several long scans in right ascension were made through the ridge, as described below. Repeated measurements of the position of peak flux density at the core of OMC-1 were used to monitor the telescope pointing; the relative positions in the map are accurate to $\pm 1'$. Flux measurements in the outer portions of the source were normalized to the repeated measurements of the OMC-1 peak to account for changes in atmospheric transmission; this relative photometry gave results which were reproducible to $\pm 10\%$. An absolute flux scale was established by measurements of the OMC-1 peak relative to Jupiter, for which the submillimeter brightness temperature was taken to be 140 K (Loewenstein *et al.* 1977; Whitcomb 1979). The calibration uncertainty as determined from the scatter in four separate determinations of the relative flux of Jupiter and the OMC-1 peak is $\pm 10\%$ for both the narrow-band and the broad-band photometry.

III. RESULTS

The present photometric results for OMC-1 and OMC-2 are combined in Figure 1 with previous far-infrared measurements made with similar fields of view. The peak flux density measured from OMC-1

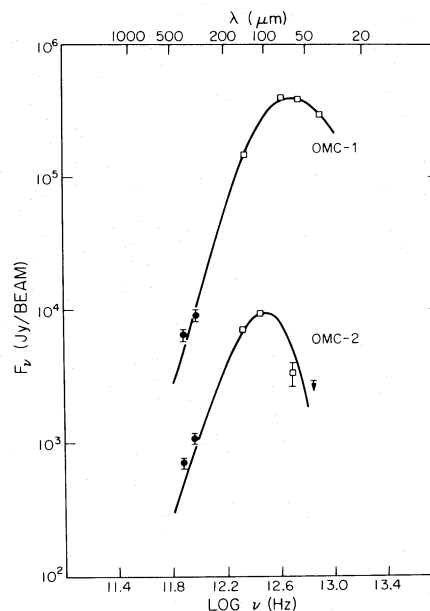


FIG. 1.—Far-infrared and submillimeter energy distributions for the peaks of OMC-1 and OMC-2 with angular fields of view about 3'. For OMC-1, a smooth curve is drawn through the data as an aid to the eye. For OMC-2, the smooth curve is computed for a grain temperature $T_g = 30 \text{ K}$, modified by a particle emission efficiency $Q(\lambda) \propto \lambda^{-2}$. Sources of data: ● (present work, 3'.0 beam); □ (Thronson *et al.* 1978, 3'.5 beam). The uncertainties in the Thronson *et al.* data are less than 10% except where indicated.

into the 3'.0 beam is $9200 \pm 900 \text{ Jy}$ at 340 μm and $6700 \pm 700 \text{ Jy}$ at 400 μm ; the corresponding flux densities measured at the position of OMC-2 are $1100 \pm 100 \text{ Jy}$ and $720 \pm 70 \text{ Jy}$. The submillimeter radiation is interpreted as continuum emission from dust, since the photometry of Figure 1 shows a thermal spectrum. No other known emission mechanism is likely to affect the measurements significantly. At OMC-1, the expected free-free emission is $\lesssim 5\%$ of the observed flux (see, e.g., Goss and Shaver 1970), and unresolved line emission from ^{12}CO and other molecules can be estimated to be $\lesssim 10\%$ of the observed submillimeter flux throughout the region mapped.

Figure 2 shows the map of the submillimeter emission from the core of L1641. The map is dominated by a maximum at OMC-1 and a continuous narrow ridge extending around 30' (5 pc) north-south. In the north-south direction, the emission from the vicinity of OMC-1 is resolved with a width of $\sim 6'$. The surface brightness of the ridge north of OMC-1 is about 10% of the peak value; note that a discrete emission feature is not observed at OMC-2.

To investigate the effects of flux in the reference beams on the appearance of the ridge, seven scans $\geq 20'$ long in right ascension were made through the ridge at roughly uniform spacing in declination. To compute the width of the ridge, these observed scans were compared with model scans obtained by convolving the telescope beam profile with a model ridge

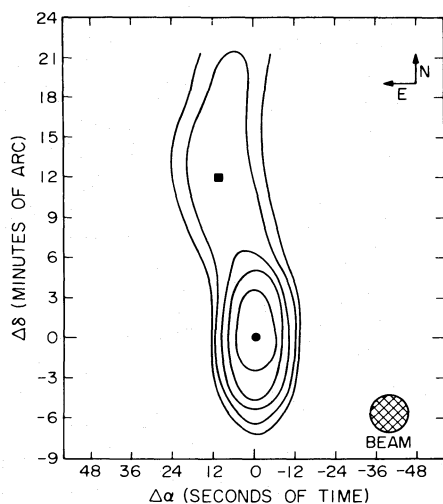


FIG. 2.—Map of L1641 near the Orion Nebula at $400 \mu\text{m}$. The contour spacing is logarithmic at levels of 0.03, 0.06, 0.12, 0.25, and 0.50 times the peak flux density at the position of OMC-1, which is 6700 Jy into a 3.0 beam; the corresponding peak surface brightness is $7.8 \times 10^{-17} \text{ W m}^{-2} \text{ Hz}^{-1} \text{ sr}^{-1}$ for a uniform source. The lowest contour is at the 3σ level. The coordinates are relative to the position of peak emission at OMC-1 ($\alpha_{1950} = 5^{\text{h}}32^{\text{m}}47^{\text{s}}$, $\delta = -5^{\circ}24'30''$). The central positions of OMC-1 and OMC-2 are indicated by the circle and the square, respectively.

which is of infinite north-south extent and which has a Gaussian east-west shape. The results indicate that the directly measured peak flux densities (Fig. 4a) are not significantly affected by flux in the reference beams and that the full width at half-maximum of the ridge is $\lesssim 3'$ in the southern portion near OMC-1 and $\sim 5'$ in the northern portion. For the purposes of constructing the contour map of Figure 2 and of calculating the total flux densities and dust masses, $3'$ was used for the ridge width within $6'$ of OMC-1; farther north, $5'$ was used. It is found in this way that the total $400 \mu\text{m}$ flux density from OMC-1 and the ridge to the north is $2.1 \times 10^4 \text{ Jy}$; of this, about 30% is emitted by dust which is farther than $7'$ north of OMC-1.

Table 1 lists the submillimeter flux densities observed at OMC-1 and OMC-2. Also listed for the same positions are a number of quantities, derived from the submillimeter observations, which are in-

dicative of the physical properties of the dust clouds. The derivation and significance of these quantities are discussed in the table and in the text below; the values tabulated for OMC-2 are typical of those for much of the ridge to the north of OMC-1. In computing these quantities, and throughout this paper, the distance to L1641 is taken to be 0.5 kpc .

In Figure 3, the $400 \mu\text{m}$ map of the core of L1641 is compared with molecular and thermal radio continuum maps of the same region. A ridge of comparable extent to that seen at $400 \mu\text{m}$ is apparent in ^{13}CO ($J = 1-0$) observations with similar angular resolution (see Figs. 3a, b). In contrast to the similarity of the distributions of dust and molecular emission, the radio continuum observations at 5 GHz (Fig. 3c) indicate a clumpy north-south distribution for the H II regions. This shows that the dust observed in emission at $400 \mu\text{m}$ is associated with the molecular clouds rather than with the H II regions.

IV. DISCUSSION

a) Relative Mass Distribution along the Ridge

If the submillimeter emission is due to thermal emission from dust, the observed flux can be related to the mass of emitting dust. The submillimeter optical depth τ of a dust cloud is

$$\tau = N_g Q \pi a^2, \quad (1)$$

where N_g is the column number density of grains, a is the characteristic grain radius, and Q is the $400 \mu\text{m}$ absorption efficiency. For particles which are small compared with the wavelength under consideration, as is assumed to be the case here, the ratio Q/a is independent of a and depends only on the grain material. In this case, equation (1) can be rewritten as

$$\tau = D \left(\frac{3}{4\rho} \right) \left(\frac{Q}{a} \right), \quad (2)$$

where D is the mass column density of grains, and ρ is the bulk density of the grain material.

It follows from equation (2) that the flux observed from a cloud which is optically thin, as is the case for L1641 (see Table 1), is equal to

$$F = \frac{100 M_g}{GR^2(e^{36/T_g} - 1)}, \quad (3)$$

TABLE 1
PROPERTIES OF OMC-1 AND OMC-2 DUST CLOUDS

Name	Position	$F_{400 \mu\text{m}}$ (Jy)	T_g (K)	M_g (M_{\odot})	τ	D (g cm^{-2})
OMC-1.....	$\alpha_{1950} = 5^{\text{h}}32^{\text{m}}47^{\text{s}}$ $\delta_{1950} = -5^{\circ}24'30''$	6700	45	4.4	1.5×10^{-2}	4.1×10^{-3}
OMC-2.....	$\alpha_{1950} = 5^{\text{h}}32^{\text{m}}59^{\text{s}}.5$ $\delta_{1950} = -5^{\circ}12'30''$	720	30	0.9	3.1×10^{-3}	8.3×10^{-4}

NOTE.— $F_{400 \mu\text{m}}$ is measured $400 \mu\text{m}$ flux density into 3.0 beam. T_g is grain temperature from far-infrared observations (Thronson *et al.* 1978) assuming $Q(\lambda) \propto \lambda^{-2}$ for the particle emission efficiency. M_g is mass of dust within one 3.0 beam. The $400 \mu\text{m}$ optical depth, τ , and the dust column density, D , are averages over the beam, assuming a uniform source. The tabulated values for OMC-2 are typical for the portion of the ridge between $10'$ and $22'$ north of OMC-1.

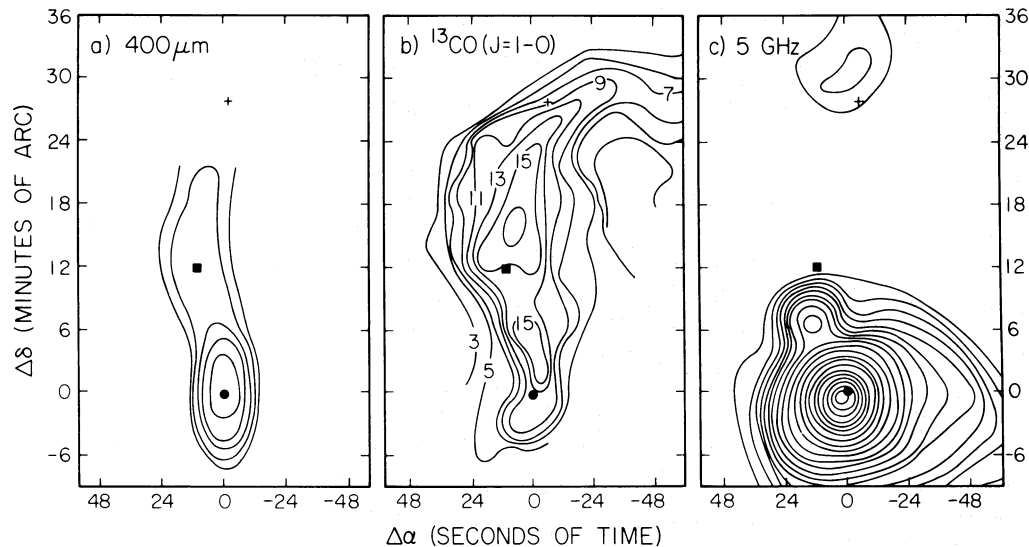


FIG. 3.—Emission from dust and gas as observed from the center of L1641. On each map, the positions of OMC-1, OMC-2, and OMC-3 are indicated by a filled circle, a filled square, and a cross, respectively. (a) The $400\ \mu\text{m}$ dust continuum emission map also shown in Fig. 2. (b) The ^{13}CO ($J = 1-0$) peak radiation temperature map observed by Kutner, Evans, and Tucker (1976) at 2.6 resolution. (c) The contour map of brightness temperature at $5\ \text{GHz}$ observed by Goss and Shaver (1970) at 4.0 resolution. The peak brightness temperature near OMC-1 is $184\ \text{K}$, and the peak brightness temperature just north of OMC-3 is $0.75\ \text{K}$.

where F is the observed $400\ \mu\text{m}$ flux density in Jy, M_g is the mass of dust in M_\odot , T_g is the dust grain temperature in K, and R is the distance to the cloud in kpc. The grain properties are included in the quantity $G \equiv \rho a/Q$. Note that $G = 3/(4k)$, where k ($\text{cm}^2\ \text{g}^{-1}$) is the bulk mass absorption coefficient of the grain material. Figure 4a shows the observed distribution of $400\ \mu\text{m}$ flux density along the central north-south ridge of the L1641 cloud. This can be converted to a dust mass distribution by the use of equation (3) if the temperature structure of the cloud is known.

Much of the information on the dust temperatures adopted for use in equation (3) is based on far-infrared measurements at several points along the ridge. The smooth curve interpolated between the measured temperatures plotted in Figure 4b is the temperature distribution used for the analysis between OMC-1 and OMC-2; the temperature is observed to decrease smoothly away from the vicinity of OMC-1. North of OMC-2 and south of OMC-1 the temperature distribution is chosen so as to exhibit the slow spatial variation in temperature expected in an optically thin cosmic dust cloud (Scoville and Kwan 1976; see also the analysis by Keene *et al.* 1980). The general character of the temperature distribution in Figure 4b is consistent with more recent measurements (Keene *et al.* 1980; Werner *et al.* 1980).

The dust mass distribution given in Figure 4c is calculated using equation (3) and the data of Figures 4a and 4b. Because of the slow variation of T_g expected along the ridge (Fig. 4b) and also because the exponential term in equation (3) is not very large for the range of T_g considered, the calculated mass distribution should be insensitive to the details of the assumptions about T_g . Thus Figure 4c gives an

accurate representation of the relative distribution of dust mass along the ridge, provided that the grain constant G is independent of T_g . As discussed in § IVb below, a value of $G = 0.2\ \text{g cm}^{-2}$ has been adopted for the determination of absolute dust masses, which range from 0.1 to $4.4\ M_\odot$ per $3'$ beam. A total dust mass of $25\ M_\odot$ is derived for the core of L1641. Because the sensitivity of the present observations decreases for emission from distributions of dust which are uniform on angular scales greater than $5'$, the above mass estimate refers only to the region of $400\ \mu\text{m}$ emission shown in Figure 2 and not to the entire region mapped in ^{13}CO by Kutner, Evans, and Tucker (1976) (see Fig. 3b), which may contain considerably more than $25\ M_\odot$ of dust.

Figure 4 shows that the dust mass distribution follows closely the distribution of the submillimeter emission. Therefore the central region of L1641 contains a dense core of dust clouds about $5'$ wide and $30'$ long. The maximum column density occurs at OMC-1; a broad secondary maximum is seen $5'$ north of OMC-2 where the column density is about one-third of the OMC-1 value.

Figure 4c shows a minimum in the dust column density $\sim 7'$ north of the center of OMC-1. Therefore the mass distribution suggests that the ridge consists of two condensations. One is centered at OMC-1 and the other is centered $\sim 5'$ north of OMC-2. Each condensation has a north-south size of $\sim 1-2\ \text{pc}$, and integration of Figure 4c shows that each contains $\sim 12\ M_\odot$ of dust. Based on their molecular line observations, Kutner, Evans, and Tucker (1976) have also found evidence for a minimum in the column density of matter $\sim 7'$ north of OMC-1.

On a finer spatial scale, the distribution of dust along the ridge is very smooth. There is no evidence

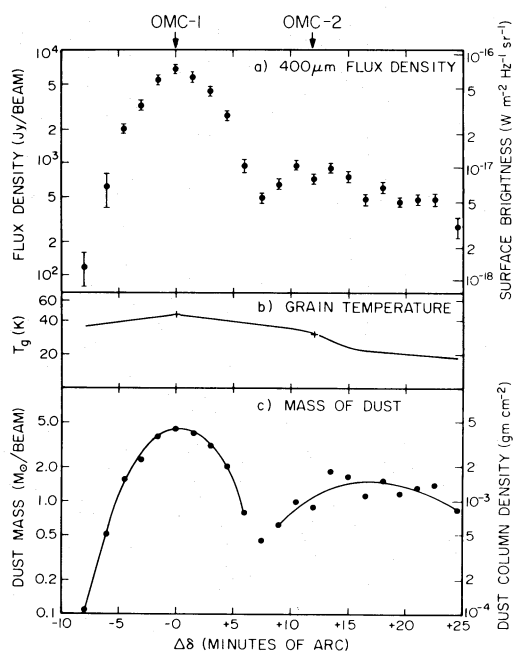


FIG. 4.—(a) The distribution of $400\ \mu\text{m}$ flux density versus declination along the central ridge of L1641. The plotted data are measurements at the right ascension of OMC-1 for $\Delta\delta \leq 6'$ and 2.5' to the east for $\Delta\delta \geq 7.5'$. The declination offset is given with respect to the declination of OMC-1 ($\delta_{1,950} = -5^{\circ}24'30''$). The positions of OMC-1 and OMC-2 are indicated at the top of the panel. Each plotted point is the mean of three to five separate observations. The left-hand axis gives the flux in Jy per 3.0 beam, and the right-hand axis gives the corresponding surface brightness, assuming a uniform source filling the beam. (b) Temperature distribution along the central ridge of L1641. The crosses show the dust temperature as determined at OMC-1 and OMC-2 by fitting a gray-body curve modified by a $Q(\lambda) \propto \lambda^{-2}$ emissivity law to the 3.5 resolution infrared photometry of Thronson *et al.* (1978). The smooth curve shows the model temperature distribution adopted for the ridge. (c) The distribution of dust mass along the central ridge of L1641. The dust mass is computed from the observed $400\ \mu\text{m}$ flux density (a) using the temperature distribution given in (b) and equation (1) of the text. The left-hand axis gives the dust mass in M_{\odot} per 3.0 beam, and the right-hand axis gives the column density of dust assuming a uniform source filling the beam. The solid lines indicate the two dust condensations discussed in the text.

in Figure 4c for unresolved condensations of dust which would be suggestive of clumping or fragmentation at the ~ 0.5 pc spatial scale of the present observations. The limit which can be set on the mass of such condensations varies along the ridge, but Figure 4c suggests that a single unresolved clump containing $\geq 2 M_{\odot}$ of dust would stand out prominently in the northern portion of the ridge.

b) Properties of the Dust

Loren (1980) has recently mapped a large area of the L1641 cloud in the $J = 1-0$ lines of ^{12}CO and ^{13}CO with 2.6' resolution; he has analyzed the data to produce a complete ^{13}CO column density map of the region. On this ^{13}CO column density map, a north-south ridge is seen which is strikingly similar in

shape, orientation, and extent to the ridge of dust inferred from the present submillimeter observations. The similarity emphasizes the fact that the dust observed in emission at $400\ \mu\text{m}$ is intimately associated with the molecular gas. A relationship between submillimeter optical depth and molecular column density can be inferred from a comparison of the dust continuum and ^{13}CO observations (see, e.g., Righini-Cohen and Simon 1977) and used to estimate some properties of the dust grains. For this purpose, measurements from 10' to 22' N of OMC-1 are used. This region is well suited for this analysis, since the ^{13}CO column density, the dust temperature, and the submillimeter flux are smoothly varying; the grain parameters derived below for the OMC-2 condensation will therefore be adopted for later reports of the survey.

The results of Loren (1980), based on an LTE analysis, show that the values of the ^{13}CO column density, N_{13} , lie in the range $5-7 \times 10^{16}\ \text{cm}^{-2}$ for this region. The submillimeter optical depth, τ , is determined by comparing the observed submillimeter surface brightness at each point with that of a blackbody of temperature T_g .

A value of τ/N_{13} has been computed at each of nine points evenly spaced along the central ridge of the OMC-2 condensation. The scatter in the values of the ratio is $\pm 30\%$ around a mean value

$$\left(\frac{\tau}{N_{13}}\right)_{\text{mean}} = 8 \times 10^{-20}\ \text{cm}^2. \quad (4)$$

This value is close to that derived by Righini-Cohen and Simon (1977) for OMC-2, but significantly lower than the average value they derive from 1' resolution observations of the cores of a group of molecular clouds.

Equation (4) can be used to derive information about the grains provided that the ratio of N_{13} to the molecular hydrogen column density, N_{H_2} , is known. This ratio may vary from one galactic molecular cloud to another (see, for example, Wootten *et al.* 1978), but

$$N_{13}/N_{\text{H}_2} = 2 \times 10^{-6} \quad (5)$$

is adopted from the LTE analysis of Dickman (1978) for clouds of somewhat lower density than those studied here. Equations (4) and (5) imply

$$\tau/N_{\text{H}_2} = 1.6 \times 10^{-25}\ \text{cm}^2. \quad (6)$$

Using equations (2) and (6), and assuming a dust-to-gas ratio by mass of 1%,

$$G = \frac{\rho a}{Q} = 0.2. \quad (7)$$

This value was used in § IVa to determine the absolute scale of dust masses. The corresponding bulk mass absorption coefficient is given by

$$k = 3/(4G) = 4\ \text{cm}^2\ \text{g}^{-1}.$$

Finally, taking a nominal value of $\rho = 1 \text{ g cm}^{-3}$, we find from equation (7) that $(Q/a) = 5 \text{ cm}^{-1}$.

Although these estimates for Q/a and k are rough, the estimated values are of the same order of magnitude as is measured or calculated for a number of plausible grain materials at this wavelength (Aannestad 1975; Day 1976). These calculations also predict that the particle absorption efficiency $Q(\lambda)$ will vary with wavelength λ as $Q(\lambda) \propto \lambda^{-1.5}$ to $\lambda^{-3.5}$ at submillimeter wavelengths; the energy distributions in Figure 1 are consistent with this. Also note that the grains must emit much less efficiently than implied by equation (7) if the value $N_{13}/N_{\text{H}_2} = 3 \times 10^{-8}$ derived by Wootten *et al.* (1978) for the peak of OMC-2 is applicable to the entire northern portion of the ridge.

The value for τ/N_{H_2} derived above for the northern portion of the ridge can be used to estimate the column density of matter through the center of OMC-1 where the interpretation of the molecular data could be complicated by optical depth effects. The submillimeter optical depth at OMC-1 is 0.015; from equation (6), this predicts an average molecular column density $N_{\text{H}_2} \approx 10^{23} \text{ cm}^{-2}$ over the central 3' of OMC-1. This agrees reasonably well with the value $N_{\text{H}_2} \approx 2 \times 10^{23} \text{ cm}^{-2}$ derived by Evans *et al.* (1975) for the same region on the basis of 2 cm H_2CO observations.

c) Energetics

The present data emphasize some of the general properties of the energetics of the dust clouds in the dense core of L1641 (see also Keene *et al.* 1980). First, the present results show that the grains which are radiating at submillimeter wavelengths are probably heated by infrared rather than by visual or ultraviolet radiation. For the diffuse interstellar medium, the grain optical depth at visual wavelengths, τ_v , is related to the hydrogen nucleus column density N_{H} (cm^{-2}) by

$$\tau_v = 5 \times 10^{-22} N_{\text{H}} \quad (8)$$

(Bohlin, Savage, and Drake 1978). Together, equations (6) and (8) imply $\tau_v = 6 \times 10^3 \tau$. Thus for a typical point in the dense core of L1641, where $\tau \approx 3.1 \times 10^{-3}$ (Table 1), the optical depth of the cloud at visual wavelengths is ~ 20 . Even with some allowance for the uncertainties in the derivation of equation (6) and in the applicability of equation (8) to molecular regions, it is likely that the dust clouds are opaque at optical and ultraviolet wavelengths. Therefore most of the grains in the cloud interior are heated by the penetrating infrared radiation reradiated by the grains closest to the heating sources; this is true whether the heating sources are embedded within the cloud or external to it.

The present submillimeter measurements and the distribution of temperatures shown in Figure 4b can be used to estimate the luminosity of the dust clouds to the north of OMC-1. For each point along the ridge, the far-infrared luminosity is estimated by integrating the thermal energy distribution correspond-

ing to the temperature shown in Figure 4b, modified by a wavelength-dependent optical depth $\tau_\lambda \propto \lambda^{-2}$, which is normalized to the observed 400 μm optical depth. When calculated this way, the far-infrared luminosity of the ridge between 7.5 and 25' N of the center of OMC-1 is $\sim 3 \times 10^4 L_\odot$ or $\sim 8\%$ of the luminosity observed for the OMC-1 region (Keene *et al.* 1980). Thus the thermal emission from the northern portion of the ridge probably does not represent a large fraction of the total far-infrared luminosity of L1641. Note also that the submillimeter ($\lambda \gtrsim 400 \mu\text{m}$) luminosity of the entire ridge (Fig. 2) is $\sim 500 L_\odot$, which is less than 1% of the total luminosity emitted by the dust clouds.

V. CONCLUSIONS

Submillimeter continuum emission from dust has been mapped over the central $\sim 30'$ of the L1641 cloud, which includes the OMC-1 and OMC-2 regions. The low optical depth of the emitting region at submillimeter wavelengths has permitted a reliable determination of the relative spatial distribution of the dust in this region, largely independent of the calibration uncertainties and of the assumptions required to derive the absolute dust density. The analysis shows that L1641 has an elongated high density core with dimensions ~ 5 pc north-south by ~ 0.8 pc east-west, extending northward from OMC-1, which is the position of maximum dust column density.

The present submillimeter observations suggest that the dense core of L1641 consists of two condensations of comparable dust mass ($\sim 12 M_\odot$) and north-south size (~ 1 – 2 pc); one is centered at OMC-1 and the other is centered about 5' north of OMC-2. Each condensation is opaque at visual and ultraviolet wavelengths. No evidence for smaller condensations is seen down to the resolution limit of the present observations, which is ~ 0.5 pc.

The distribution of dust is very similar to the distribution of molecular gas in this region, which also exhibits a pronounced north-south ridge; this shows that the dust is located in the molecular clouds. Based on a comparison of molecular and dust continuum emission from the northern portion of the ridge where these quantities are slowly varying, a value $(\tau/N_{13}) = 8 \times 10^{-20} \text{ cm}^2$ is derived for the ratio of 400 μm optical depth to ^{13}CO column density in the molecular cloud.

The initial installation of the 1.6 m telescope at White Mountain was carried out by D. Gezari, with the help of E. Becklin and G. Forrester, who also participated in the earliest observing programs. We thank R. Leighton and G. Neugebauer for making the 1.6 m telescope available for this project and for advice concerning its use; in addition, we acknowledge the assistance and support of G. Neugebauer and W. J. Welch with many other aspects of this program. L. Anderson and D. Harlow assisted with the observations, and M. Raff contributed in many ways to the

development of the observatory and the success of this project. We thank I. Gatley and B. T. Soifer for important suggestions concerning the observing program and the analysis of the data, N. Evans and R. Loren for making their molecular observations available to us and for commenting on the manuscript, and M. Kutner for valuable comments. Finally,

we wish to thank the staff of the White Mountain Research Station, especially D. Buser and N. Pace, for supporting these astronomical observations so energetically. This work was supported by NSF grants AST 76-81092 and AST 73-04908 to the California Institute of Technology and NSF grant AST 76-22480 to the University of California.

REFERENCES

- Aannestad, P. A. 1975, *Ap. J.*, **200**, 30.
 Bohlin, R. C., Savage, B. D., and Drake, J. F. 1978, *Ap. J.*, **224**, 132.
 Day, K. L. 1976, *Ap. J.*, **210**, 614.
 Dickman, R. 1978, *Ap. J. Suppl.*, **37**, 407.
 Evans, N. J., II, Zuckerman, B., Sato, T., and Morris, G. 1975, *Ap. J.*, **199**, 383.
 Fazio, G. G., Kleinmann, D. E., Noyes, R. W., Wright, E. L., Zeilik, M. I., and Low, F. J. 1974, *Ap. J. (Letters)*, **192**, L33.
 Gatley, I., Becklin, E. E., Matthews, K., Neugebauer, G., Penston, M. V., and Scoville, N. 1974, *Ap. J. (Letters)*, **191**, L121.
 Gezari, D. Y., Joyce, R. R., Righini, G., and Simon, M. 1974, *Ap. J. (Letters)*, **191**, L33.
 Goss, W. M., and Shaver, P. A. 1970, *Australian J. Phys., Ap. Suppl.*, No. 14, p. 1.
 Harper, D. A., Jr., Low, F. J., Rieke, G., and Armstrong, K. R. 1972, *Ap. J. (Letters)*, **177**, L21.
 Hauser, M. G., and Notaries, H. A. 1975, *Bull. AAS*, **7**, 409.
 Hudson, H. S., and Soifer, B. T. 1976, *Ap. J.*, **206**, 100.
 Keene, J., Smith, J. R., Harper, D. A., Hildebrand, R., and Whitcomb, S. 1980, in preparation.
 Kutner, M. L., Evans, N. J., II, and Tucker, K. C. 1976, *Ap. J.*, **209**, 452.
 Kutner, M. L., Tucker, K. D., Chin, G., and Thaddeus, P. 1977, *Ap. J.*, **215**, 521.
 Loewenstein, R. F., *et al.* 1977, *Icarus*, **31**, 315.
 Loren, R. 1980, in preparation.
 Lynds, B. T. 1962, *Ap. J. Suppl.*, **7**, 1.
 Muehlner, D., and Weiss, R. 1973, *Phys. Rev. D*, **7**, 326.
 Neugebauer, G., and Leighton, R. B. 1969, *Two-Micron Sky Survey—A Preliminary Catalog* (NASA SP-3047).
 Righini-Cohen, G., and Simon, M. 1977, *Ap. J.*, **213**, 390.
 Scoville, N. Z., and Kwan, J. 1976, *Ap. J.*, **206**, 718.
 Soifer, B. T., and Hudson, H. S. 1974, *Ap. J. (Letters)*, **191**, L83.
 Smith, J. R., Cudaback, D. D., and Lynch, D. K. 1980, in preparation.
 Thronson, H. A., Jr., Harper, D. A., Keene, J., Loewenstein, R. F., Moseley, H., and Telesco, C. M. 1978, *A.J.*, **83**, 492.
 Werner, M. W., Becklin, E. E., Ennis, D., Gatley, I., Neugebauer, G., and Sellgren, K. 1980, in preparation.
 Werner, M. W., Becklin, E. E., and Neugebauer, G. 1977, *Science*, **197**, 723.
 Whitcomb, S. 1979, private communication.
 Wootten, A., Evans, N. J., Snell, R., and Vanden Bout, P. 1978, *Ap. J. (Letters)*, **225**, L143.

D. D. CUDABACK: Radio Astronomy Laboratory, University of California, Berkeley, CA 94720

D. K. LYNCH: Hughes Research Laboratories, 3011 Malibu Canyon Road, Malibu, CA 90265

J. R. SMITH: Yerkes Observatory, Williams Bay, WI 53191

M. W. WERNER: Space Science Division, NASA Ames Research Center, Moffett Field, CA 94035